HHS Public Access

Author manuscript

ACS Chem Biol. Author manuscript; available in PMC 2018 July 21.

Published in final edited form as:

ACS Chem Biol. 2017 July 21; 12(7): 1737–1742. doi:10.1021/acschembio.7b00130.

Real-Time *in Vivo* Detection of H_2O_2 Using Hyperpolarized ^{13}C-Thiourea

Arif Wibowo[†], **Jae Mo Park**[‡,§], **Shie-Chau Liu**[§], **Chaitan Khosla**[†,∥,⊥], and **Daniel M. Spielman**[§]

[†]Department of Biochemistry, Stanford University, Stanford, California 94305, United States

[‡]Advanced Imaging Research Center, University of Texas Southwestern Medical Center, Dallas, Texas 75390, United States

[§]Department of Radiology, Stanford University, Stanford, California 94305, United States

[∥]Department of Chemistry, Stanford University, Stanford, California 94305, United States

[⊥]Stanford ChEM-H, Stanford University, Stanford, California 94305, United Stat3es

Abstract

Reactive oxygen species (ROS) are essential cellular metabolites widely implicated in many diseases including cancer, inflammation, and cardiovascular and neurodegenerative disorders. Yet, ROS signaling remains poorly understood, and their measurements are a challenge due to high reactivity and instability. Here, we report the development of ^{13}C-thiourea as a probe to detect and measure H_2O_2 dynamics with high sensitivity and spatiotemporal resolution using hyperpolarized ^{13}C magnetic resonance spectroscopic imaging. In particular, we show ^{13}C-thiourea to be highly polarizable and to possess a long spin–lattice relaxation time (T_1), which enables real-time monitoring of ROS-mediated transformation. We also demonstrate that ^{13}C-thiourea reacts readily with H_2O_2 to give chemically distinguishable products *in vitro* and validate their detection *in vivo* in a mouse liver. This study suggests that ^{13}C-thiourea is a promising agent for noninvasive detection of H_2O_2 *in vivo*. More broadly, our findings outline a viable clinical application for H_2O_2 detection in patients with a range of diseases.

Graphical abstract

Correspondence to: Daniel M. Spielman.

Supporting Information: The Supporting Information is available free of charge on the ACS Publications website at DOI: 10.1021/acschem-bio.7b00130.

Detailed methods include selectivity assays, NMR spectroscopy, kinetic measurement, polarization procedures, spectral measurement and imaging (PDF)

Notes: The authors declare no competing financial interest.

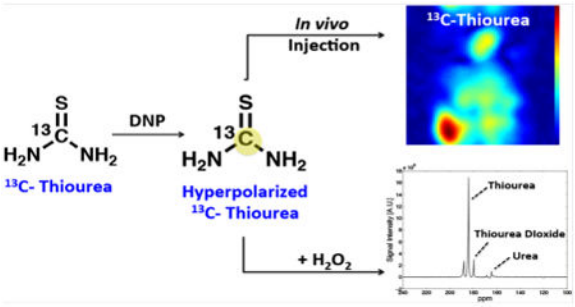

Oxidative stress is a hallmark of many pathophysiological diseases corresponding to the oxidative damage incurred by aberrant reactive oxygen species (ROS) production. These ROS are essential for cellular signaling.[1,2] They include highly reactive oxygen metabolites such as hydrogen peroxide (H_2O_2), superoxide ($O_2^{\bullet-}$), and hydroxyl radical (^{-}OH). Dysregulation of ROS homeostasis leads to oxidative stress and irreversible molecular damage, which is associated with various disease states such as cancer, inflammation, and cardiovascular and neurodegenerative disorders.[3–7]

Despite their importance, the precise mechanisms of ROS signaling are poorly understood. The high reactivity and short lifetime of ROS have further complicated efforts for determining their spatiotemporal dynamics *in vivo*. ROS detection in biological systems therefore requires probes that rapidly react with ROS to produce stable quantifiable products. Indeed, several studies have reported the development of ROS-specific probes for live *in vivo* optical detection.[8,9] These probes capitalized on the enhanced contrast of a caged fluorescence emission that is activated upon ROS-induced transformation. The use of small molecule and nanoparticle probes in these studies has in turn, inspired us to exploit ^{13}C magnetic resonance spectroscopic imaging (MRSI)[10] to study ROS flux *in vivo*.

In contrast to optical techniques, MRSI enables noninvasive acquisition of deep-tissue images *in vivo* and the investigation of real-time cellular metabolism with high spatial and temporal resolution.[11,12] However, MRSI experiments have inherently low sensitivity and are therefore limited to the detection of abundant ^{1}H nuclei from water molecules and lipid chains *in vivo*. To gain information on intermediary cellular metabolites and their fluxes, we have utilized ^{13}C MRSI by taking advantage of its wide chemical shift differences to encompass signals from both a substrate and its metabolic product(s).[10] To overcome the naturally low abundance of a ^{13}C signal, we hyperpolarized the ^{13}C-labeled substrate by using dynamic nuclear polarization (DNP) to afford more than 10 000-fold signal enhancement of the ^{13}C-probe and its subsequent metabolic products.[13,14] In combination with a rapid dissolution process, hyperpolarized (HP) ^{13}C-substrates such as [1-^{13}C]-pyruvate,[15] [2-^{13}C]-pyruvate,[16] [^{13}C]-glucose,[17] [^{13}C]-bicarbonate,[18] [2-^{13}C]-fruc-tose,[19] and [2-^{13}C]-dihydroxyacetone[20] have been used as metabolic probes to investigate cellular metabolism with high spectral resolution. Notably, [1-^{13}C]-dehydroascorbate (DHA)[21,22] and [1-^{13}C]-benzoylformic acid (BFA)[23] have been reported as HP ^{13}C-substrates to probe oxidative stress specific to redox and H_2O_2 sensing, respectively.

To design new HP ^{13}C-probes for ROS detection in vivo, we focused on small-molecule metabolites exhibiting several key properties. First, the substrate should be highly polarizable either by DNP or other methods.[24–26] Second, both the substrate and its metabolic product(s) should possess a long spin–lattice relaxation time (T_1), as needed for robust *in vivo* detection. Third, the HP probe should reveal a distinctive chemical shift for its ^{13}C nuclei upon reaction with ROS in order to allow spectroscopic detection of both the probe and its products. Finally, the probe should be nontoxic (at micromolar to millimolar concentration) and be rapidly transported for ROS-mediated reaction (or react in the extracellular space).

To this end, we explored ^{13}C-thiourea (^{13}C-TU) as an HP probe for ROS detection. Thiourea is a water-soluble ROS scavenger that has been associated with antioxidant proper-ties.[27,28] In liver microsomes, flavin-containing monooxygenases (FMO) catalyze an NADPH-dependent S-oxygenation of thiourea in the presence of O_2,[29] leading to the formation of formamidine sulfenic acids (TUO) that in turn either react reversibly with glutathione (GSH) or undergo further oxidation to form thiourea dioxide (TUO_2). Notably, no thiourea transporters have been identified in mammals, even though studies have implicated urea transporters for a shared transport mechanism with thiourea in erythrocytes.[30] In addition, saturation kinetics in perfused rat inner medullary collecting duct showed saturation of the urea transporter with a K_M = 20 mM for thiourea.[31] Moreover, studies on a single intra-peritoneal exposure of thiourea in different animal models have yielded a range of lethal dose (LD_{50}) concentrations of up to 1340 mg/kg body weight in rats.[32] Together, these studies suggest that ^{13}C-TU is an attractive HP probe candidate for ROS detection.

To test our hypothesis, we determined the selectivity of ^{13}C-TU with different ROS that are responsible for many cellular signaling events. These ROS have been implicated in oxidative damage inflicted on fatty acid, DNA, and proteins as well as other cellular components (Figure 1A).[33] Briefly, thiourea was exposed to several biologically relevant ROS for 10 min, and the formation of oxidized products was monitored by ^{13}C NMR. In the presence of $^{\bullet}$OOH (H_2O_2 or tBuOOH), we detected oxidation of TU (δ184 ppm) to form TUO_2 (δ 179.5 ppm), as identified by LC-MS (Figure 1B and S1). When reacted with other ROS such as superoxide ($O_2^{\bullet-}$) and hydroxyl radical ($^{\bullet}$OH), thiourea remained unchanged. Reaction with hypochlorite ($^{-}$OCl) and peroxynitrite ($ONOO^-$) yielded urea (δ 165 ppm) as the hydrolyzed byproduct (Figure 1B and C). While *in vitro* oxidation of thiourea is not limited to peroxide, we were especially interested in using ^{13}C-TU to detect H_2O_2 in vivo due to its central role in cellular signaling.[34,35] Such a measurement is physiologically relevant because FMO-mediated oxygenation of thiourea in vivo is reported to proceed via reaction with H_2O_2.[36] We therefore investigated thiourea oxidation by reacting different concentrations of H_2O_2 (2-27 μM) with 10 μM ^{13}C-TU and examining ^{13}C-TUO_2 formation by ^{13}C NMR (Figure 1D). By plotting the ratio of the integrated ^{13}C-TUO_2 product peak to the total signal intensities (^{13}C-TU + ^{13}C-TUO_2) against peroxide, we showed a good linear correlation to increasing H_2O_2 concentration (Figure 1E) and confirmed its sensitivity for detecting low micromolar peroxide concentration *in vitro*.

Next, we sought to measure the rate of thiourea oxidation by H_2O_2 using UV/vis spectroscopy. We first performed a UV sweep of thiourea solutions (12.5–200 μM) and

determined a maximum absorbance at λ_{max} = 237 nm with an extinction coefficient ε = 0.0113 μM^{-1} cm^{-1} (Figure S2). We measured the kinetics of thiourea oxidation by detecting A_{237} change (depletion of thiourea) when reacted with H_2O_2. Briefly, two thiourea solutions (0.0625 and 0.125 mM) were prepared in a buffered solution at pH 7.4, incubated with different H_2O_2 concentrations (0.125–8 mM), and monitored for change in A_{237} over 50 min (Figure 2A). By plotting the initial rate against peroxide concentration, we found the results to be in close agreement with a previous report,[37] that the rate of thiourea oxidation is first-order with respect to each thiourea and H_2O_2 concentrations (Figure 2B). Kinetics measurements reveal that the reaction between thiourea and H_2O_2 proceeds rapidly to produce thiourea dioxide with a second-order rate constant (k_2) of 0.082 ± 0.002 M^{-1} s^{-1} (Figures 2B and S3).

We then proceeded to test the ability of ^{13}C-TU to undergo hyperpolarization using a preclinical HyperSense (Oxford Instruments) and a clinical SPINlab (GE Healthcare) polarizer. The polarization of a ^{13}C-labeled substrate exploits the principle of the nuclear Overhauser effect, which transfers nuclear spin polarization from one spin bath to another (e.g., free radical species to the ^{13}C nuclei of thiourea) using microwave irradiation at near absolute zero temperature (1.2 K for HyperSense, 0.8 K for SPINlab). The hyperpolarized sample was then rapidly dissolved, and the corresponding T_1 measured with a clinical 3T MRI scanner. Samples polarized with the HyperSense exhibited a polarization level of 3.2 ± 0.1% and T_1 = 30.2 ± 0.8 s, while the SPINlab produced a polarization level of 10.4 ± 1.1% and T_1 = 53.8 ± 3.7 s (Figure 3a and Figure S4). Notably, higher polarization of the sample from the SPINlab might be attributed to the use of a hand-held electromagnetic carrier, which preserves polarization during sample transfer,[38] and the longer T_1 measurement was due to the exclusion of gadolinium. Together, polarization by the HyperSense and SPINlab represented a 12 200- and 39 500-fold enhancement, respectively, of the ^{13}C-TU signals relative to thermal equilibrium. We then evaluated ^{13}C-TU for spectroscopic detection of H_2O_2 *in vitro* by characterizing its oxidation product(s) with ^{13}C-MRS. Briefly, 4 M solutions of ^{13}C-TU and 15 mM of OX063 (Oxford Instruments) radicals in 60% (v/v) glycerol were hyperpolarized at 1.2 K and irradiated with microwaves (139.88 GHz) using a HyperSense polarizer. After hyperpolarization, the sample was rapidly dissolved in 100 mM Trizma-HCl buffer (pH ~ 7.6) to a final thiourea concentration of 50 mM and reacted with 50 μM H_2O_2 for ~30 s before spectral acquisition with a 3T scanner. Representative spectra from the peroxide-treated ^{13}C-TU showed several distinct peaks. In particular, we identified ^{13}C-TUO_2 (179.6 ppm) as the oxidation product of ^{13}C-TU (184 ppm) within 50 s of H_2O_2 reaction (Figure 3B and C). Additional byproducts of TU oxidation were also detected at 164.5 and 168.7 ppm, which were assigned to ^{13}C-urea and ^{13}C-TU_2, respectively.[39] Resonance frequencies of TU and the oxidized products are assigned based on the resonance of a 1 M ^{13}C-bicarbonate phantom. Indeed, peroxide-mediated oxidation of TU proceeds via a mono-oxygenated intermediate (TUO), which further oxidizes to TUO_2. Additionaly, the TUO intermediates may undergo reversible disulfide (TU_2) formation in the presence of excess TU.[40] Any resulting TUO_2 can then be readily hydrolyzed to form urea under mildly basic conditions.[40] Finally, we observed a previously unidentified peak at 188.1 ppm, which likely corresponds to the ^{13}C-TUO intermediate. Indeed, time course analysis of the reaction revealed a nonlinear decay in ^{13}C-

TUO signal at t = 35–40 s, which was followed by an increase in the ^{13}C-TUO$_2$ signal at t = 50 s (Figure 3C, Figure S5). In contrast, a linear decay was observed in ^{13}C-TU as a result of the spin–lattice relaxation time of the hyperpolarized signal (Figure S5). These findings suggest that despite the spin-lattice relaxation time, we were able to detect ^{13}C-TUO oxidation to ^{13}C-TUO$_2$ in real time. Together, these results demonstrate that the identification of a transient ^{13}C-TUO intermediate is required for ^{13}C-TUO$_2$ production and that TU can successfully detect H_2O_2 by ^{13}C-MRS.

To evaluate TU for in vivo H_2O_2 sensing, we applied HP ^{13}C-TU to detect the endogenous H_2O_2 level in healthy male rats. Briefly, 4 M solutions of ^{13}C-TU and 15 mM AH111501 (GE Healthcare) radicals were hyperpolarized using a SPINlab polarizer, rapidly dissolved into 50 mM final thiourea concentration and intravenously injected into an anesthetized rat for imaging with a 3T MR scanner. A slice-selective ^{13}C spectroscopic image over an oblique plane encompassing several major organs was acquired with free induction decay chemical shift imaging sequence using a ^{13}C/^{1}H dual-tuned volume coil (FID CSI, field of view = 80 × 80 mm^2, matrix size = 16 × 16, flip angle = 10°, acquisition time = 19 s, repetition time = 75 ms), and the corresponding ^{1}H MRI confirmed significant ^{13}C-TU resonance in well-perfused tissues of a rat, particularly in the heart, liver, and kidney (Figure 4A). However, no metabolic products from thiourea oxidation were detected above the noise level, presumably due to native antioxidant responses that kept endogenous H_2O_2 concentration low (~10^{-8} M)[41] and thus undetectable by our HP probe. To assess whether thiourea oxidation could be detected in vivo, we coinjected HP ^{13}C-TU with H_2O_2 into the intraperitoneal cavity of an anesthetized mouse to simulate elevated ROS level under oxidative stress. A small transmit/ receive surface radiofrequency coil was then used for localized data acquisition from the mouse liver, and a ^{13}C-MRS scan of the injection site revealed several oxidized species in the liver (Figure 4B). One major oxidative product detected downfield of ^{13}C-TU (184 ppm) was identified as the mono-oxygenated ^{13}C-TUO intermediate (188.1 ppm). Moreover, several smaller but detectable oxidative products were assigned to ^{13}C-TUO$_2$ (179.5 ppm), ^{13}C-urea (164.5 ppm), and ^{13}C-TU$_2$ (168.1 ppm) based on their *in vitro* chemical shifts. Both ^{13}C-TUO and ^{13}C-TUO$_2$ exhibited a linear rate of decay in vivo with apparent rate constants (1/T_1) of k_{TUO} = 0.0342 s^{-1} and k_{TUO2} = 0.0249 s^{-1}, respectively, which were similar to ^{13}C-TU decay (k_{TU} = 0.0308 s^{-1}; Figure 4c). In addition, we examined the extent of thiourea oxidation by calculating the relative TUO$_2$/TUO ratios *in vitro* and *in vivo* and found that the relative TUO$_2$ signal is 7.9-fold lower *in vivo*. These results suggest that ^{13}C-TUO was not actively oxidized to ^{13}C-TUO$_2$ *in vivo* despite the exogenous peroxide addition and that the lack of *in vivo* oxidation of ^{13}C-TUO might be attributed to the rapid antioxidant response to clear any excess peroxide.

In summary, we have introduced a potential new ^{13}C-MRSI probe to detect ROS level in real-time. Indeed, the present studies represent an ongoing effort to measure oxidative stress noninvasively. Our data demonstrate that ^{13}C-TU may be a viable ^{13}C-MRSI agent with important applications for real-time H_2O_2 detection. Notably, we were successful in detecting thiourea oxidation products in vivo using hyperpolarized ^{13}C-TU and coinjected H_2O_2. In addition, we found the highest ^{13}C-TU resonance in well-perfused organs, implicating its potential use for extracellular ROS measurements in blood and/or plasma.

Future studies with ^{13}C-TU in diseased animal models may provide important insights into the role of oxidative stress in pathophysiology.

Supplementary Material

Refer to Web version on PubMed Central for supplementary material.

Acknowledgments

This work is dedicated to the memory of Dr. G. Sommer.

Funding: This work was supported by NIH grants R01 EB019018, DK063158, S10 OD012283, and P41 EB015891; DOD CDMRP PC100427; the Gambhir-RSL grant; and the Stanford BioX program.

References

1. D'Autréaux B, Toledano MB. ROS as signalling mole- cules: mechanisms that generate specificity in ROS homeostasis. Nat Rev Mol Cell Biol. 2007; 8:813–824. [PubMed: 17848967]
2. Giorgio M, Trinei M, Migliaccio E, Pelicci PG. Hydrogen peroxide: a metabolic by-product or a common mediator of ageing signals? Nat Rev Mol Cell Biol. 2007; 8:722–778. [PubMed: 17700625]
3. Diehn M, Cho RW, Lobo NA, Kalisky T, Dorie MJ, Kulp AN, Qian D, Lam JS, Alles LE, Wong M, Joshua B, Kaplan MJ, Wapnir I, Dirbas FM, Somlo G, Garberoglio C, Paz B, Shen J, Lau SK, Quake SR, Brown JM, Weissman IL, Clarke MF. Association of reactive oxygen species levels and radioresistance in cancer stem cells. Nature. 2009; 458:780–783. [PubMed: 19194462]
4. Weinberg F, Hamanaka R, Wheaton WW, Weinberg S, Joseph J, Lopez M, Kalyanaraman B, Mutlu GM, Budinger GR, Chandel NS. Mitochondrial metabolism and ROS generation are essential for Kras-mediated tumorigenicity. Proc Natl Acad Sci U S A. 2010; 107:8788–8793. [PubMed: 20421486]
5. Zhou R, Yazdi AS, Menu P, Tschopp J. A role for mitochondria in NLRP3 inflammasome activation. Nature. 2011; 469:221–225. [PubMed: 21124315]
6. Brown DI, Griendling KK. Regulation of signal transduction by reactive oxygen species in the cardiovascular system. Circ Res. 2015; 116:531–549. [PubMed: 25634975]
7. Lin MT, Beal MF. Mitochondrial dysfunction and oxidative stress in neurodegenerative diseases. Nature. 2006; 443:787–795. [PubMed: 17051205]
8. Shuhendler AJ, Pu K, Cui L, Uetrecht JP, Rao J. Real-time imaging of oxidative and nitrosative stress in the liver of live animals for drug-toxicity testing. Nat Biotechnol. 2014; 32:373–380. [PubMed: 24658645]
9. Van de Bittner GC, Dubikovskaya EA, Bertozzi CR, Chang CJ. In vivo imaging of hydrogen peroxide production in a murine tumor model with a chemoselective bioluminescent reporter. Proc Natl Acad Sci U S A. 2010; 107:21316–21321. [PubMed: 21115844]
10. Shulman RG, Rothman DL. 13C NMR of intermediary metabolism: implications for systemic physiology. Annu Rev Physiol. 2001; 63:15–48. [PubMed: 11181947]
11. Gadian DG, Radda GK. NMR studies of tissue metabolism. Annu Rev Biochem. 1981; 50:69–83. [PubMed: 7023368]
12. van der Graaf M. In vivo magnetic resonancespectroscopy: basic methodology and clinical applications. Eur Biophys J. 2010; 39:527–540. [PubMed: 19680645]
13. Ardenkjaer-Larsen JH, Fridlund B, Gram A, Hansson G, Hansson L, Lerche MH, Servin R, Thaning M, Golman K. Increase of signal-to-noise ratio of more than 10,000 times in liquid state NMR. Proc Natl Acad Sci U S A. 2003; 100:10158–10163. [PubMed: 12930897]
14. Golman K, Ardenkjaer-Larsen JH, Petersson JS, Mansson S, Leunbach I. Molecular imaging with endogenous substances. Proc Natl Acad Sci U S A. 2003; 100:10435–10439. [PubMed: 12930896]

15. Mayer D, Yen YF, Tropp J, Pfefferbaum A, Hurd RE, Spielman DM. Application of subsecond spiral chemical shift imaging to real-time multislice metabolic imaging of the rat in vivo after injection of hyperpolarized 13C1-pyruvate. Magn Reson Med. 2009; 62:557–564. [PubMed: 19585607]
16. Park JM, Josan S, Grafendorfer T, Yen YF, Hurd RE, Spielman DM, Mayer D. Measuring mitochondrial metabolism in rat brain in vivo using MR Spectroscopy of hyperpolarized [2-C-13]pyruvate. NMR Biomed. 2013; 26:1197–1203. [PubMed: 23553852]
17. Rodrigues TB, Serrao EM, Kennedy BW, Hu DE, Kettunen MI, Brindle KM. Magnetic resonance imaging of tumor glycolysis using hyperpolarized C-labeled glucose. Nat Med. 2013; 20:93–97. [PubMed: 24317119]
18. Korenchan DE, Flavell RR, Baligand C, Sriram R, Neumann K, Sukumar S, VanBrocklin H, Vigneron DB, Wilson DM, Kurhanewicz J. Dynamic nuclear polarization ofbiocompatible 13C-enriched carbonates for in vivo pH imaging. Chem Commun. 2016; 52:3030–3033.
19. Keshari KR, Wilson DM, Chen AP, Bok R, Larson PE, Hu S, Van Criekinge M, Macdonald JM, Vigneron DB, Kurhanewicz J. Hyperpolarized [2-^{13}C]-Fructose: A Hemik et al DNP Substrate for In Vivo Metabolic Imaging. J Am Chem Soc. 2009; 131:17591–17596. [PubMed: 19860409]
20. Marco-Rius I, von Morze C, Sriram R, Cao P, Chang GY, Milshteyn E, Bok RA, Ohliger MA, Pearce D, Kurhanewicz J, Larson PE, Vigneron DB, Merritt M. Monitoring acute metabolic changes in the liver and kidneys induced by fructose and glucose using hyperpolarized [2-13 C]dihydroxyacetone. Magn Reson Med. 2017; 77:65–73. [PubMed: 27859575]
21. Keshari KR, Kurhanewicz J, Bok R, Larson PE, Vigneron DB, Wilson DM. Hyperpolarized 13C dehydroascorbate as an endogenous redox sensor for in vivo metabolic imaging. Proc Natl Acad Sci U S A. 2011; 108:18606–18611. [PubMed: 22042839]
22. Bohndiek SE, Kettunen MI, Hu DE, Kennedy BWC, Boren J, Gallagher FA, Brindle KM. Hyperpolarized [1-^{13}C]-Ascorbic and Dehydroascorbic Acid: Vitamin C as a Probe for Imaging Redox Status in Vivo. J Am Chem Soc. 2011; 133:11795–11801. [PubMed: 21692446]
23. Lippert AR, Keshari KR, Kurhanewicz J, Chang CJ. A hydrogen peroxide-responsive hyperpolarized ^{13}C MRI contrast agent. J Am Chem Soc. 2011; 133:3776–3779. [PubMed: 21366297]
24. Schroder L, Lowery TJ, Hilty C, Wemmer DE, Pines A. Molecular imaging using a targeted magnetic resonance hyperpolarized biosensor. Science. 2006; 314:446–449. [PubMed: 17053143]
25. Bowers CR, Weitekamp DP. Parahydrogen and synthesis allow dramatically enhanced nuclear alignment. J Am Chem Soc. 1987; 109:5541–5542.
26. Reineri F, Santelia D, Viale A, Cerutti E, Poggi L, Tichy T, Premkumar SSD, Gobetto R, Aime S. Para-hydrogenated Glucose Derivatives as Potential 13C-Hyperpolarized Probes for Magnetic Resonance Imaging. J Am Chem Soc. 2010; 132:7186–7193. [PubMed: 20441193]
27. Doroshow JH. Role of hydrogen peroxide andhydroxyl radical formation in the killing of Ehrlich tumor cells byanticancer quinones. Proc Natl Acad Sci U S A. 1986; 83:4514–4518. [PubMed: 3086887]
28. Takeyama K, Dabbagh K, Jeong Shim J, Dao-Pick T, Ueki IF, Nadel JA. Oxidative stress causes mucin synthesisvia transactivation of epidermal growth factor receptor: role ofneutrophils. J Immunol. 2000; 164:1546–1552. [PubMed: 10640773]
29. Poulsen LL, Hyslop RM, Ziegler DM. S-Oxygenation of N-substituted Thioureas catalyzed by the pig liver microsomal FAD-containing monooxygenase. Arch Biochem Biophys. 1979; 198:78–88. [PubMed: 507850]
30. Zhao D, Sonawane ND, Levin MH, Yang B. Comparative transport efficiencies of urea analogues through urea transporter UT-B. Biochim miophys Acta, Biomembr. 2007; 1768:1815–1821.
31. Chou CL, Sands JM, Nonoguchi H, Knepper MA. Concentration dependence of urea and thiourea transport pathway in rat inner medullary collecting duct. Am J Physiol. 1990; 258:486–494.
32. Ziegler-Skylakakis, K. Concise International Chemical Assessment Document 49: Thiourea. World Health Organization; Geneva: 2003.
33. Halliwell, B., Gutteridge, JMC. Free Radicals in Biology and Medicine. 5th. Oxford University Press; Oxford; 2015.

34. Rhee SG. Cell signaling. H_2O_2, a necessary evil for cell signaling. Science. 2006; 312:1882–1883. [PubMed: 16809515]

35. Paulsen CE, Carroll KS. Orchestrating redox signaling networks through regulatory cysteine switches. ACS Chem Biol. 2010; 5:47–62. [PubMed: 19957967]

36. Siddens LK, Krueger SK, Henderson MC, Williams DE. Mammalian flavin-containing monooxygenase (FMO) as a source of hydrogen peroxide. Biochem Pharmacol. 2014; 89:141–147. [PubMed: 24561181]

37. Hoffmann M, Edwards JO. Kinetics andmechanism of the oxidation of thiourea and N, N′-dialkylthioureas byhydrogen peroxide. Inorg Chem. 1977; 16:3333–3338.

38. Shang H, Skloss T, von Morze C, Carvajal L, Van Criekinge M, Milshteyn E, Larson PE, Hurd RE, Vigneron DB. Handheld electromagnet carrier for transfer of hyperpolarizedcarbon-13 samples. Magn Reson Med. 2016; 75:917–922. [PubMed: 25765516]

39. Arifoglu MA, Marmer WN, Dudley RB. Reaction of thiourea with hydrogen peroxide: ^{13}C NMR studies of anoxidative/reductive bleaching process. Text Res J. 1992; 62:94–100.

40. Makarov SV, Horvath AK, Silaghi-Dumitrescu R, Gao Q. Recent Developments in the Chemistry of Thiourea Oxides. Chem - Eur J. 2014; 20:14164–14176. [PubMed: 25265917]

41. Giorgio M, Trinei M, Migliaccio E, Pelicci PG. Hydrogen peroxide: a metabolic by-product or a common mediator of ageing signals? Nat Rev Mol Cell Biol. 2007; 8:722–728. [PubMed: 17700625]

Abbreviations

HP	hyperpolarized
TU	thiourea
TUO	formamidine sulfenic acid
TUO_2	thiourea dioxide
MRS	magnetic resonance spectroscopy
MRSI	magnetic resonance spectroscopic imaging

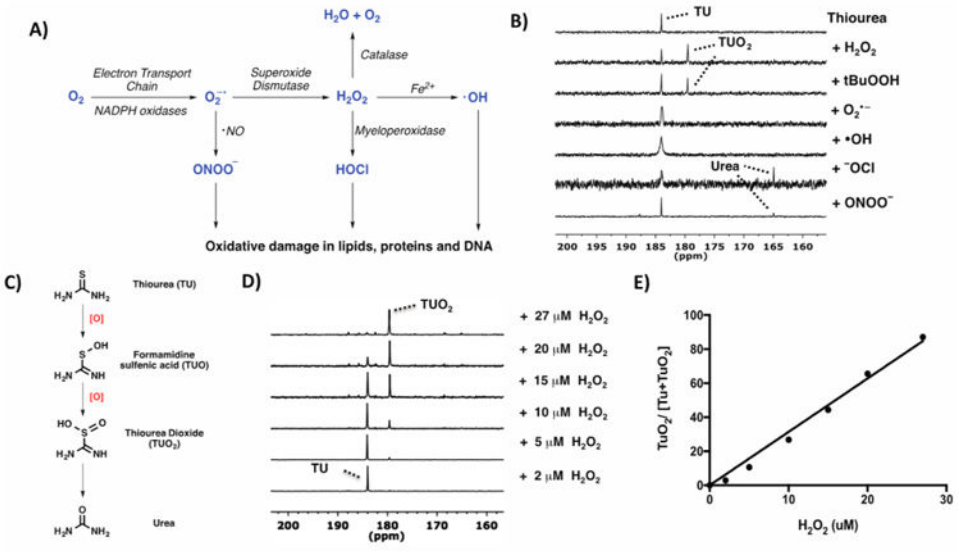

Figure 1.

(A) Different kinds of ROS generated via multiple enzymatic steps. (B) Response of thiourea (TU) to various ROS at thermal equilibrium. All ROS (H_2O_2, tBuOOH, NaONOO, and NaOCl) were added to TU in D_2O (except for KO_2-treated sample in DMSO) and the spectra recorded with ^{13}C NMR at 125 mHz. Reaction with H_2O_2 and tBuOOH yielded thiourea dioxide (TUO_2) as the oxidized product. (C) TU was oxidized to TUO_2 before getting hydrolyzed to urea. (D) ^{13}C NMR spectra of 10 μM ^{13}C-TU after 10 min reaction with various concentrations of H_2O_2 (2–27 μM). (E) Linear correlation of the ratio of integrated peak intensities of ^{13}C-TUO_2 to the total signal intensities (^{13}C-TU + ^{13}C-TUO_2) against H_2O_2 concentration, $R^2 = 0.994$.

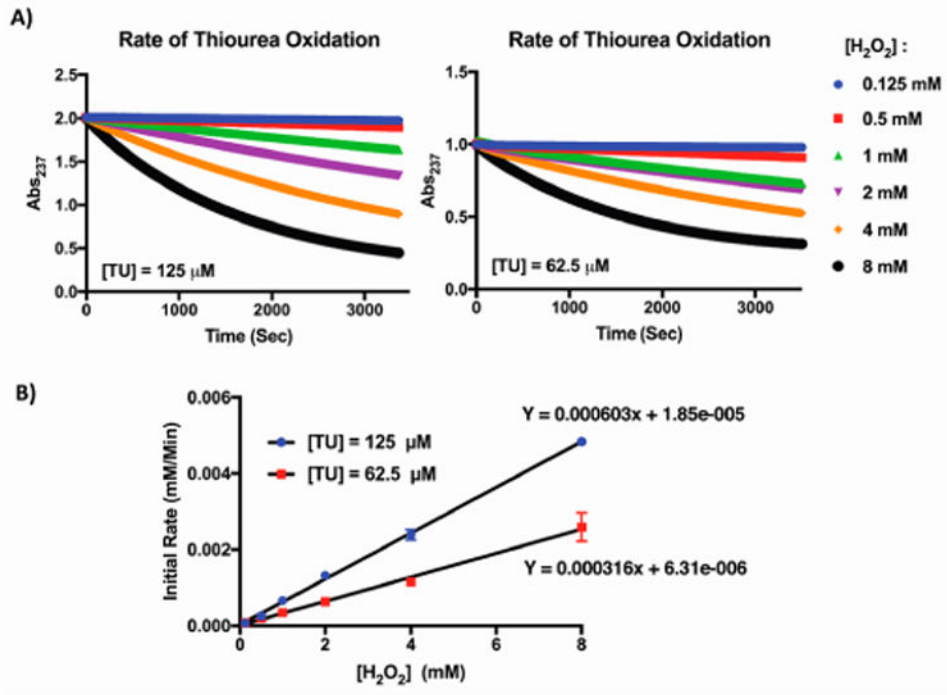

Figure 2.

(A) UV/vis measurement of TU oxidation with H_2O_2. Representative measurement of thiourea consumption with different H_2O_2 concentrations (0.125–8 mM) as measured by A_{237} change. (B) Oxidation follows a first order reaction kinetic with respect to TU and H_2O_2. Second-order rate constant, $k_2 = 0.082 \pm 0.002\ M^{-1}\ s^{-1}$.

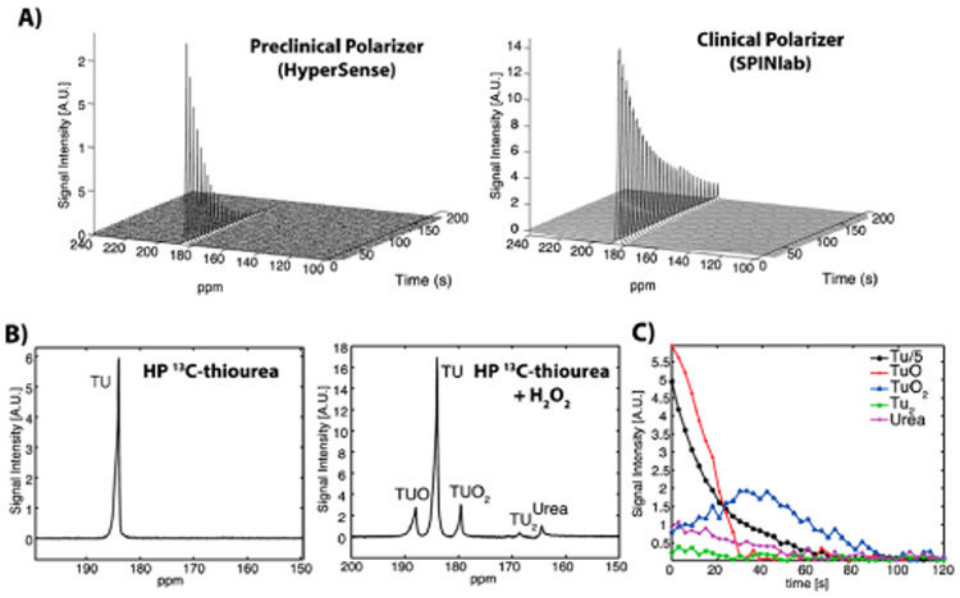

Figure 3.

In vitro ^{13}C MR spectra of hyperpolarized TU. (A) ^{13}C-TU was hyperpolarized using a HyperSense (preclinical) or a SPINlab (clinical) polarizer. Polarization and T_1 of the hyperpolarized TU samples were measured using a clinical 3T MR scanner and a nonselective pulse-and-acquire MRS sequence (flip-angle = 5.625°, temporal resolution = 3 s) after a 30 s delay from the dissolution due to mixing of ^{13}C-TU with H_2O_2 and transfer to the magnet. (B) Time-averaged spectra of hyperpolarized ^{13}C-TU showed multiple oxidation products (TUO, TUO_2, TU_2, and urea) when reacted with 50 μM H_2O_2. (C) Temporal changes of hyperpolarized TU and products due to T_1 decay and the reaction to H_2O_2 were detected from time courses of hyperpolarized ^{13}C TU and the oxidation products. See SI for experimental details.

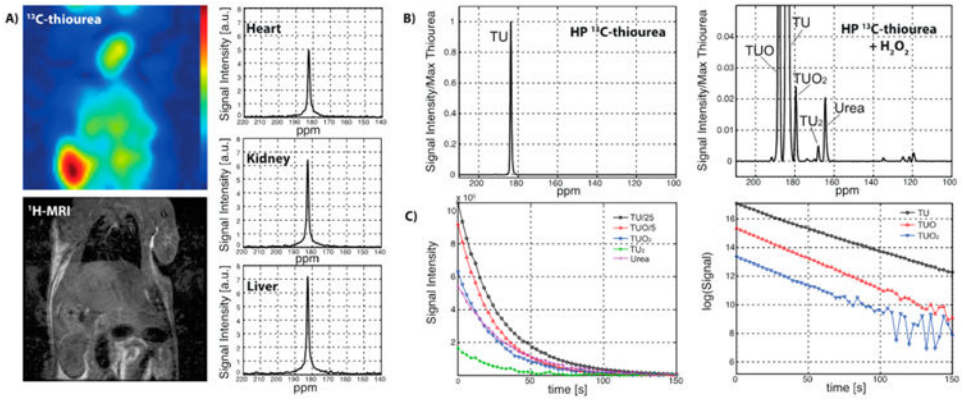

Figure 4.

In vivo detection of hyperpolarized ^{13}C-TU. (A) A slice-selective 2D ^{13}C chemical shift imaging (CSI) and a ^{1}H MRI over an oblique plane that contains heart, kidney, and liver of a healthy rat, acquired using a ^{13}C/^{1}H dual-tuned volume coil. The CSI scan started 20 s after a bolus injection (i.v.) of hyperpolarized ^{13}C-TU, estimating the spatial distribution of the TU and measuring its perfusion into each organ (field of view = 80 × 80 mm^2, matrix size = 16 × 16, slice thickness = 15 mm). No ^{13}C-oxidized product was observed. (B) ^{13}C-MR spectra of a mouse liver after an injection (i.p.) of hyperpolarized ^{13}C-TU with and without H_2O_2. A nonselective pulse-and-acquire MRS sequence was used (flip-angle = 10°, temporal resolution = 3 s). The localization was achieved by positioning a small ^{13}C transmit/receive surface coil (diameter = 28 mm) on top of the mouse liver and the intraperitoneal cavity. Oxidized products (TUO and TUO_2) and byproducts (TU_2 and urea) were detected *in vivo* immediately when TU and H_2O_2 were coinjected. No oxidized product was observed with the TU-only injection. (C) All the hyperpolarized signals of ^{13}C-metabolites exhibited monoexponential decays as a result of the spin–lattice relaxations (T_1). See SI for experimental details.